

Nonlinear evolution of spherical perturbation in the Universe with cosmological constant and quintessence

Ewa L. Łokas¹ and Yehuda Hoffman²

¹*Copernicus Astronomical Center, Bartycka 18, 00–716 Warsaw, Poland*

²*Racah Institute of Physics, Hebrew University, Jerusalem 91904, Israel*

26 April 2024

ABSTRACT

We generalize the spherical collapse model for the formation of bound objects to apply in a Universe with cosmological constant and quintessence. We calculate the critical condition for collapse of an overdense region and give exact values of the characteristic densities and redshifts of its evolution. We apply the results to calculate the mass function of bound objects. Comparison with the data for clusters indicates a preference of models with quintessence over those with cosmological constant.

Key words: methods: analytical – cosmology: theory – galaxies: clusters general – galaxies: formation – large-scale structure of Universe

1 INTRODUCTION

The spherical collapse model was first developed by Gunn & Gott (1972) for a flat Universe with no cosmological constant. It assumes that the process of formation of bound objects in the Universe can be at first approximation described by evolution of an uniformly overdense spherical region in otherwise smooth background (and it is therefore called the top hat model). Despite its simplicity, the model is still widely used to explain properties of a single bound object via extensions such as the spherical infall model (Gunn 1977; Hoffman & Shaham 1985; Łokas 2000) as well as statistical properties of different classes of objects via Press-Schechter-like formalisms (Press & Schechter 1974, hereafter PS; Lacey & Cole 1993, 1994).

Recently, our knowledge on background cosmology has improved dramatically due to new supernovae and cosmic microwave background data. Current observations favor a flat Universe with $\Omega_0 = 0.3$ (see e.g. Harun-or-Rashid & Roos 2001 and references therein) and the remaining contribution in the form of cosmological constant or some other form of dark energy. A new class of models that satisfy these observational constraints has been proposed by Caldwell, Dave, & Steinhardt (1998) where the cosmological constant is replaced with an energy component characterized by the equation of state $p/\rho = w \neq -1$. The component can cluster on largest scales and therefore affect the mass power spectrum (Ma et al. 1999) and microwave background anisotropies (Balbi et al. 2001; Doran et al. 2000).

A considerable effort has gone into attempts to put constraints on models with quintessence and presently the values of $-1 < w < -0.6$ seem most feasible observationally (Wang et al. 2000; Huterer & Turner 2000). Another di-

rection of investigations is into physical basis for the existence of such component with the oldest attempts going back to Ratra & Peebles (1988). One of the promising models is based on so-called “tracker fields” that display an attractor-like behavior causing the energy density of quintessence to follow the radiation density in the radiation dominated era but dominate over matter density after matter-radiation equality (Zlatev, Wang, & Steinhardt 1999; Steinhardt, Wang, & Zlatev 1999). It is still debated, however, how w should depend on time, and whether its redshift dependence can be reliably determined observationally (Barger & Marfatia 2001; Maor, Brustein, & Steinhardt 2001; Weller & Albrecht 2001).

From the gravitational instability point of view the quintessence field and the cosmological constant play a very similar role, both can be treated as (unclustered) dark energy components that differ by their equation of state parameter, w . Technically, the equations governing the expansion of the Universe and the growth of density perturbations in the two models differ only by the value of w . Throughout the paper we aim at providing a unified treatment of both models, considering the quintessence model to be a generalization of the cosmological constant model.

Given the growing popularity of models with cosmological constant or quintessence we generalize the description of the spherical collapse to include its effect. The top hat model serves as a basic tool in performing analytic calculations of structure formation via gravitational instability in an expanding Universe, most notably in the framework of the PS formalism. Our aim here is to extend the arsenal of analytical, or quasi-analytical, formulae describing the redshifts and (over)densities characterizing the collapse processes to the case of a Universe dominated by a cosmological constant

or quintessence field. We derive some simple analytical formulae and fits that will serve as useful tools in constructing models of structure and galaxy formation.

The paper is organized as follows. In Section 2 we briefly summarize the properties of the cosmological model with quintessence including the linear growth factor of density fluctuations. Section 3 is devoted to the evolution of the overdense region and gives the critical threshold for collapse. Sections 4 and 5 discuss the characteristic densities of the forming object and redshifts of evolution. In Section 6 we apply the predictions of the model to calculate the cumulative mass function of clusters. The discussion follows in Section 7.

2 THE COSMOLOGICAL MODEL

Quintessence obeys the following equation of state relating its density ϱ_Q and pressure p_Q

$$p_Q = w\varrho_Q, \quad \text{where } -1 \leq w < 0. \quad (1)$$

The case of $w = -1$ corresponds to the usually defined cosmological constant.

The evolution of the scale factor $a = R/R_0 = 1/(1+z)$ (normalized to unity at present) in the quintessential Universe is governed by the Friedmann equation

$$\frac{da}{dt} = \frac{H_0}{f(a)} \quad (2)$$

where

$$f(a) = \left[1 + \Omega_0 \left(\frac{1}{a} - 1 \right) + q_0 \left(\frac{1}{a^{1+3w}} - 1 \right) \right]^{-1/2} \quad (3)$$

and H_0 is the present value of the Hubble parameter. The quantities with subscript 0 here and below denote the present values. The parameter Ω is the standard measure of the amount of matter in units of critical density and q measures the density of quintessence in the same units

$$q = \frac{\varrho_Q}{\varrho_{\text{crit}}}. \quad (4)$$

For $w = -1$ we will replace q with $\lambda = \Lambda/(3H^2)$ where $\Lambda = \text{const}$ is the standard cosmological constant. The Einstein equation for acceleration $d^2a/dt^2 = -4\pi Ga(p + \varrho/3)$ shows that $w < -1/3$ is needed for the accelerated expansion to occur.

Solving the equation for the conservation of energy $d(\varrho_Q a^3)/da = -3p_Q a^2$ with condition (1) we get the following evolution of the density of quintessence in the general case of $w = w(a)$

$$\varrho_Q = \varrho_{Q,0} \exp \left[-3 \ln a + 3 \int_a^1 \frac{w(a) da}{a} \right] \quad (5)$$

in agreement with Caldwell et al. (1998). For $w = \text{const}$, the case considered in this paper, the formula reduces to

$$\varrho_Q = \varrho_{Q,0} a^{-3(1+w)}. \quad (6)$$

The evolution of Ω and q with redshift z is given by

$$\Omega(z) = \Omega_0 (1+z)^3 \left[\frac{H_0}{H(z)} \right]^2 \quad (7)$$

and

$$q(z) = q_0 \left[\frac{H_0}{H(z)} \right]^2 (1+z)^{3(1+w)} \quad (8)$$

where

$$\begin{aligned} \left[\frac{H(z)}{H_0} \right]^2 &= (1+z)^2 (1 + \Omega_0 z) \\ &+ q_0 (1+z)^{3(1+w)} [1 - (1+z)^{-(1+3w)}]. \end{aligned} \quad (9)$$

The linear evolution of the matter density contrast $\delta = \delta\varrho/\varrho$ is governed by equation

$$\ddot{\delta} + 2\frac{\dot{a}}{a}\dot{\delta} - 4\pi G\varrho\delta = 0 \quad (10)$$

where dots represent derivatives with respect to time. In the case of $w = -1$ and $w = -1/3$ the growing mode can be constructed in a simple form (Heath 1977; Carroll, Press, & Turner 1992)

$$D(a) = \frac{5\Omega_0}{2af(a)} \int_0^a f^3(a) da \quad (11)$$

where $f(a)$ was defined in equation (3). The expression in (11) is normalized so that for $\Omega = 1$ and $q = 0$ we have $D(a) = a$.

For some special cases one can obtain analytical expressions for $D(a)$. In the well-studied case of $q_0 = 0$ and $\Omega_0 < 1$ we have

$$\begin{aligned} D(a) &= \frac{a^{3/2}}{\Omega_0^{1/2}} \left[\left(\frac{1}{a} - 1 \right) \Omega_0 + 1 \right]^{1/2} \\ &\times {}_2F_1 \left[\frac{3}{2}, \frac{5}{2}, \frac{7}{2}, a \left(1 - \frac{1}{\Omega_0} \right) \right] \end{aligned} \quad (12)$$

which is equivalent to the better known expression given by e.g. Peebles (1980). Expression (12) is also valid for $w = -1/3$ because then the q -dependent term in (3) vanishes. For $w = -1$ and $\Omega_0 + \lambda_0 = 1$ we get

$$\begin{aligned} D(a) &= \frac{a^{3/2}}{\Omega_0^{1/2}} \left[\left(\frac{1}{a} - a^2 \right) \Omega_0 + a^2 \right]^{1/2} \\ &\times {}_2F_1 \left[\frac{5}{6}, \frac{3}{2}, \frac{11}{6}, a^3 \left(1 - \frac{1}{\Omega_0} \right) \right]. \end{aligned} \quad (13)$$

In the case of $w = -1$, for arbitrary (Ω_0, λ_0) pairs $D(a)$ is easily obtained by numerical integration in equation (11) (see also Hamilton 2001). The solutions (12) and (13) together with the numerical solution to equation (10) for $w = -2/3$ are plotted in Figure 1 for the cosmological parameters $\Omega_0 = 0.3$ and $q_0 = 0.7$.

3 EVOLUTION OF THE OVERDENSE REGION

We assume that at some time t_i corresponding to redshift z_i the region of proper radius r_i is overdense by the average $\Delta_i = \text{const}$ with respect to the background, that is it encloses a mass

$$M(r_i) = \frac{4\pi}{3} \rho_{b,i} r_i^3 (1 + \Delta_i) \quad (14)$$

where $\rho_{b,i}$ is the background density of matter at t_i .

Evolution of this region is governed by the energy equation

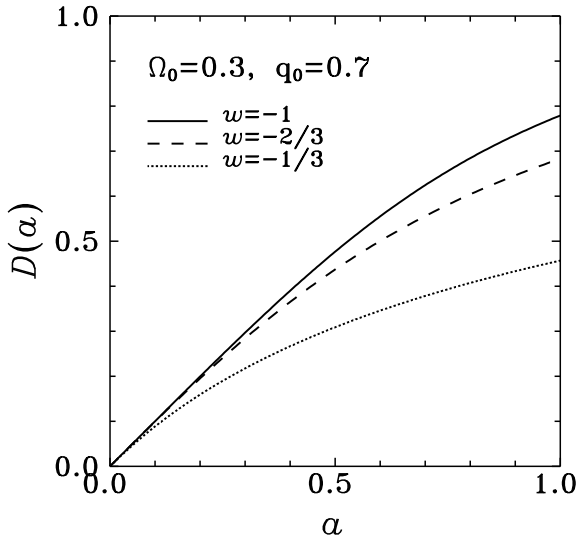


Figure 1. The linear growth rate of density fluctuations for $\Omega_0 = 0.3$, $q_0 = 0.7$ in three cases of $w = -1, -2/3$ and $-1/3$.

$$\frac{1}{2} \left(\frac{dr}{dt} \right)^2 - \frac{GM}{r} - \frac{H^2 qr^2}{2} = \varepsilon. \quad (15)$$

Expressing ε as a combination of the kinetic and potential energy per unit mass at t_i ,

$$\varepsilon(t_i) = \frac{H_i^2 r_i^2}{2} [1 - \Omega_i(1 + \Delta_i) - q_i], \quad (16)$$

using equation (14) and introducing a new variable $s = r/r_i$, equation (15) can be rewritten in the form

$$\frac{ds}{dt} = \frac{H_i}{g(a, s)} \quad (17)$$

where

$$\begin{aligned} g(a, s) &= \left\{ 1 + \Omega_i(1 + \Delta_i) \left(\frac{1}{s} - 1 \right) \right. \\ &\quad \left. + q_i \left[\left(\frac{a_i}{a} \right)^{3(1+w)} s^2 - 1 \right] \right\}^{-1/2}. \end{aligned} \quad (18)$$

In the expression above $a_i = 1/(1 + z_i)$, and the parameters $H_i = H(z_i)$, $\Omega_i = \Omega(z_i)$, $q_i = q(z_i)$ are given by equations (7)-(9).

Assuming conservation of energy we find that the maximum expansion radius r_{ta} (or equivalently, $s_{ta} = r_{ta}/r_i$) of the overdense region must obey the following condition

$$b_1 s_{ta}^3 + b_2 s_{ta} + b_3 = 0 \quad (19)$$

where

$$\begin{aligned} b_1 &= cq_i \\ b_2 &= 1 - \Omega_i(1 + \Delta_i) - q_i \\ b_3 &= \Omega_i(1 + \Delta_i) \end{aligned} \quad (20)$$

and

$$c = \left(\frac{a_i}{a_{ta}} \right)^{3(1+w)} \quad (21)$$

where a_{ta} is the scale factor at turn-around.

There are two real and positive solutions to equation (19)

$$s_{ta} = \frac{2}{\sqrt{3}} \left(\frac{-b_2}{b_1} \right)^{1/2} \cos \left(\frac{\phi - 2\pi}{3} \right) \quad (22)$$

and

$$s_{ta} = \frac{2}{\sqrt{3}} \left(\frac{-b_2}{b_1} \right)^{1/2} \cos \left(\frac{\phi}{3} \right) \quad (23)$$

where

$$\phi = \arccos \frac{x}{(x^2 + y^2)^{1/2}} \quad (24)$$

with

$$x = -9b_1^{1/2}b_3 \quad (25)$$

$$y = [3(-4b_2^3 - 27b_1b_3^2)]^{1/2}. \quad (26)$$

For $q_0 = 0$ we simply get $s_{ta} = -b_3/b_2$. The $q_0 = 0$ case is reproduced in the limit of small q_0 only by solution (22). However, although for $w = -1$ only (22) works, for higher values of w which solution is applicable depends on Ω_0 (see Subsection 4.1).

The condition for the solutions (22) and (23) to exist is

$$\Delta_i \geq \Delta_{i,cr} = \frac{1}{\Omega_i} u(q_i, c) - 1 \quad (27)$$

where

$$u(q_i, c) = 1 + \frac{(9c-4)q_i}{4} + \frac{3cq_i[8 + (9c-8)q_i]}{4v^{1/3}} + \frac{3v^{1/3}}{4} \quad (28)$$

and

$$\begin{aligned} v = v(q_i, c) &= q_i c [27c^2 q_i^2 + 36cq_i(1 - q_i) \\ &\quad + 8(1 - q_i)^2 + 8(1 - q_i)^{3/2}(1 - q_i + cq_i)^{1/2}]. \end{aligned} \quad (29)$$

In the limit of $q_0 \rightarrow 0$ we have $u(q_i) \rightarrow 1$. In this limit we reproduce the well known condition for the overdense region to turn around

$$\Delta_i > \Delta_{i,cr}(q_0 = 0) = \frac{1}{\Omega_i} - 1. \quad (30)$$

The condition (27) for the case of pure cosmological constant has been derived previously by Weinberg (1987), Martel (1991) and Lokas & Hoffman (2001). In this case of $w = -1$ we have $c = 1$ and $u(\lambda_i) > 1$ for all positive λ_0 , so the condition (27) seems more stringent than (30), i.e. in the Universe with cosmological constant overdensities have to be larger in order to collapse than in the Universe with the same density parameter Ω_i but no cosmological constant. It is more useful, however, to compare the conditions for cosmological models with the same value of the present density parameter, Ω_0 . Since the evolution of Ω depends on λ (see equation [7] and [9]), the relation between conditions (27) and (30) for a given Ω_0 is not obvious. It turns out that $\Delta_{i,cr}$ can in fact be higher as well as lower than $\Delta_{i,cr}(\lambda_0 = 0)$ depending on the choice of Ω_0 and λ_0 . The upper panel of Figure 2 shows the ratio of the two critical overdensities calculated for $z_i = 100$ as a function of Ω_0 for different values of $\lambda_0 = \text{const}$.

It is worth noting that in the case of $\lambda_0 = 0$ condition (30) is equivalent to the requirement of the energy of the overdense region to be negative. In the case of a Universe with positive λ_0 , according to equation (16) the condition $E < 0$ translates into $\Delta_i > \Omega_i^{-1}(1 - \lambda_i) - 1$ which allows densities much lower than (27) since $(1 - \lambda_i) < 1$.

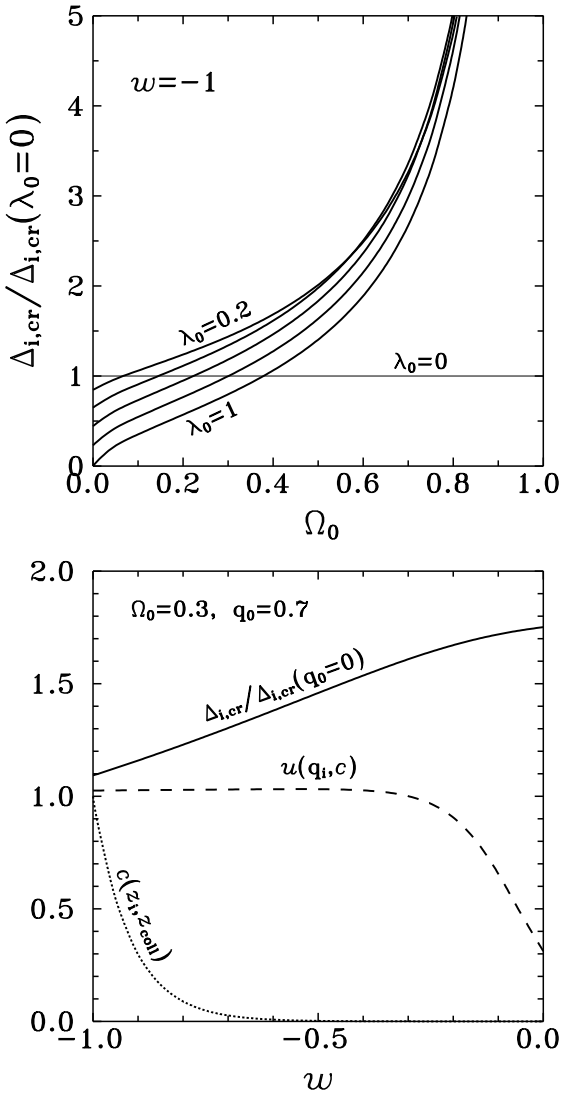


Figure 2. Upper panel: the ratio $\Delta_{i,\text{cr}}/\Delta_{i,\text{cr}}(\lambda_0 = 0)$ for $w = -1$ as a function of Ω_0 for $z_i = 100$. Solid curves from top to bottom show results for $\lambda_0 = 0.2, 0.4, 0.6, 0.8$ and 1 . The thin horizontal line marks the limiting case of $\lambda_0 = 0$, where the two overdensities are equal. Lower panel: the dependence of the quantities c , $u(q_i, c)$ and $\Delta_{i,\text{cr}}/\Delta_{i,\text{cr}}(q_0 = 0)$ on w for $\Omega_0 = 0.3$, $q_0 = 0.7$, $z_i = 100$ and $z_{\text{coll}} = 0$.

For $w > -1$, $c \neq 1$ and the critical overdensity depends not only on a_i (or z_i) but also on the scale factor at turn-around a_{ta} (see equation [21]). The dependence of the quantities c , $u(q_i, c)$ and $\Delta_{i,\text{cr}}/\Delta_{i,\text{cr}}(q_0 = 0)$ on w for $\Omega_0 = 0.3$ and $q_0 = 0.7$ is shown in the lower panel of Figure 2. We have adopted $z_i = 100$ and assumed that the collapse takes place at present, i.e. the redshift of collapse $z_{\text{coll}} = 0$ (from this condition we determine the redshift of turn around, which depends on w , see the next section).

Integrating equation (15) numerically for given w , Ω_0 and q_0 we get the trajectory $r(t)$. Figure 3 compares examples of $r(t)$ obtained for $\Omega_0 = 0.3$ and different values of w and q_0 . For the $\Omega_0 = 0.3$, $q_0 = 0$ case we have the well known analytical solutions $r/r_{\text{ta}} = (1 - \cos \theta)/2$ and $t/t_{\text{coll}} = (\theta - \sin \theta)/(2\pi)$ with $0 \leq \theta \leq 2\pi$. The plots of $r(t)$

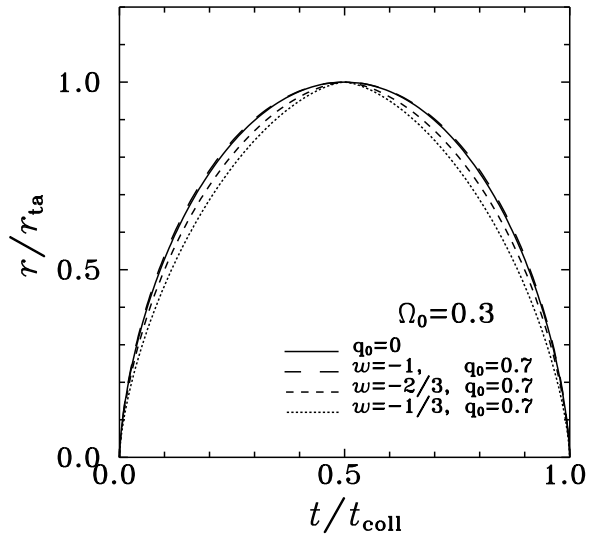


Figure 3. Evolution of radius of the presently collapsing overdense region in different models with quintessence.

shown in Figure 3 were obtained with the assumption of t_{coll} equal to the present age of Universe. In the $q_0 = 0$ case $r(t)$ is independent of the collapse time, while calculations for $q_0 \neq 0$ show that $r(t)$ approaches the $q_0 = 0$ solution for $z_{\text{coll}} \rightarrow \infty$.

4 THE CHARACTERISTIC DENSITIES

4.1 The linear density contrast at collapse

We first consider the case of pure cosmological constant, $w = -1$. We then have $g(a, s) = g(s)$ and the variables in equation (17) separate. Integrating equations (2) and (17) we get

$$\int_0^a f(a) da = H_0 t \quad (31)$$

$$\int_0^s g(s) ds = H_1 t. \quad (32)$$

Eliminating t we obtain equations which can be used to calculate the scale factor at turn-around (a_{ta}) and collapse (a_{coll}) of a region with particular Δ_i at a given z_i

$$\int_0^{a_{\text{ta}}} f(a) da = \frac{H_0}{H_1} \int_0^{s_{\text{ta}}} g(s) ds \quad (33)$$

$$\int_0^{a_{\text{coll}}} f(a) da = 2 \frac{H_0}{H_1} \int_0^{s_{\text{ta}}} g(s) ds \quad (34)$$

where s_{ta} is given by equation (22) and we defined the collapse time t_{coll} to be twice the turn-around time

$$t_{\text{ta}} = \frac{1}{H_0} \int_0^{a_{\text{ta}}} f(a) da. \quad (35)$$

Assuming that the mass inside the overdense region does not change, the overdensity inside the sphere of size r with respect to the background density at any time is

$$\delta = \frac{\rho}{\rho_b} - 1 = \frac{1}{s^3} \left(\frac{a}{a_i} \right)^3 (1 + \Delta_i) - 1 \quad (36)$$

where we used equation (14).

At early times, $t \rightarrow 0$, we can expand the expressions on the left-hand sides of equations (31)-(32) around $a = 0$ and $s = 0$ respectively. Integrating term by term we obtain

$$H_0 t = \frac{2}{3\Omega_0^{1/2}} a^{3/2} + \frac{\Omega_0 + \lambda_0 - 1}{5\Omega_0^{3/2}} a^{5/2} + O(a^{7/2}) \quad (37)$$

$$\begin{aligned} H_i t &= \frac{2}{3[\Omega_i(1 + \Delta_i)]^{1/2}} s^{3/2} \\ &+ \frac{\Omega_i(1 + \Delta_i) + \lambda_i - 1}{5[\Omega_i(1 + \Delta_i)]^{3/2}} s^{5/2} + O(s^{7/2}). \end{aligned} \quad (38)$$

Inverting both series we express a and s as power series of $t^{2/3}$

$$a = c_1 t^{2/3} + c_2 t^{4/3} + O(t^{8/3}) \quad (39)$$

where

$$\begin{aligned} c_1 &= \left(\frac{3}{2}\right)^{2/3} (H_0^2 \Omega_0)^{1/3} \\ c_2 &= \frac{3}{10} \left(\frac{3}{2}\right)^{1/3} \frac{H_0^{4/3} (1 - \Omega_0 - \lambda_0)}{\Omega_0^{1/3}}, \end{aligned}$$

and

$$s = d_1 t^{2/3} + d_2 t^{4/3} + O(t^{8/3}) \quad (40)$$

where

$$\begin{aligned} d_1 &= \left(\frac{3}{2}\right)^{2/3} [H_i^2 \Omega_i(1 + \Delta_i)]^{1/3} \\ d_2 &= \frac{3}{10} \left(\frac{3}{2}\right)^{1/3} \frac{H_i^{4/3} [1 - \Omega_i(1 + \Delta_i) - \lambda_i]}{[\Omega_i(1 + \Delta_i)]^{1/3}}. \end{aligned}$$

Inserting expressions (39) and (40) into equation (36) and keeping only the lowest order term we find

$$\begin{aligned} \delta &= \frac{3}{5} \left(\frac{3}{2}\right)^{2/3} \left[\frac{H_0^{2/3} (1 - \Omega_0 - \lambda_0)}{\Omega_0^{2/3}} \right. \\ &\quad \left. + \frac{H_i^{2/3} [\Omega_i(1 + \Delta_i) + \lambda_i - 1]}{[\Omega_i(1 + \Delta_i)]^{2/3}} \right] t^{2/3} + O(t^{4/3}). \end{aligned} \quad (41)$$

From expansion (39) we have to the lowest order $t^{2/3} = c_1^{-1} a$ so the dependence of δ on a in the limit of $a \rightarrow 0$ is

$$\delta = h(\Omega_0, \lambda_0, \Delta_i, z_i) a + O(a^2), \quad (42)$$

where

$$\begin{aligned} h(\Omega_0, \lambda_0, \Delta_i, z_i) &= \\ &= \frac{3}{5} \left[\frac{1 - \Omega_0 - \lambda_0}{\Omega_0} + \frac{[\Omega_i(1 + \Delta_i) + \lambda_i - 1](1 + z_i)}{\Omega_i(1 + \Delta_i)^{2/3}} \right]. \end{aligned} \quad (43)$$

For $w \neq -1$ the variables in equation (17) do not separate and we expand $1/g(a, s)$ for small a and s . For a given w we then find an expansion of $a(t)$ for small t analogous to (39). The presented example of $w = -1$ suggests that expansion of $s(t)$ involves the same powers of t as expansion of $a(t)$. Assuming this we introduce both expansions into equation (17) and integrate to get $s(t)$. The equation obtained this way lets us determine the coefficients of the expansion of $s(t)$. It turns out that for $-1 < w < -1/3$ the expansions and their coefficients are exactly the same as in equations (39)-(40). For $w = -1/3$ the powers of t in the expansions are the same, but coefficients are different, leading however to the same result for the density contrast (42)-(43). In the

less interesting cases of $-1/3 < w < 0$ the powers of t higher than $t^{2/3}$ in the expansions $a(t)$ and $s(t)$ are different than in (39)-(40) producing a term with the power of t lower than $2/3$ in (41) but its coefficient vanishes. It turns out that results (42)-(43) with λ replaced by q are valid for all w in the range $-1 \leq w < 0$. Using equations (7)-(9) we can rewrite h so that it does not explicitly depend on w

$$\begin{aligned} h(\Omega_0, q_0, \Delta_i, z_i) &= \\ &= \frac{3}{5} \left[\frac{1 - \Omega_0 - q_0}{\Omega_0} + \frac{\Omega_0 [1 + \Delta_i(1 + z_i)] + q_0 - 1}{\Omega_0 (1 + \Delta_i)^{2/3}} \right]. \end{aligned} \quad (44)$$

For $w = -1, -2/3, -1/3$ and arbitrary parameters (Ω_0, q_0) , one can show that

$$D(a) = a + O(a^2) \quad (45)$$

is the properly normalized solution of equation (10) around $a = 0$. Given this behavior of the linear growth factor $D(a)$, we finally obtain the density contrast as predicted by linear theory

$$\delta_L = h(\Omega_0, q_0, \Delta_i, z_i) D(a). \quad (46)$$

Note that $D(a)$ is the general solution to equation (10). The first order expansion of $D(a)$ has been used only to derive $h(\Omega_0, q_0, \Delta_i, z_i)$.

A particularly useful quantity is the linear density contrast at the moment of collapse i.e. when s reaches zero

$$\delta_c = h(\Omega_0, q_0, \Delta_i(a_{\text{coll}}), z_i) D(a_{\text{coll}}). \quad (47)$$

$\Delta_i(a_{\text{coll}})$ in the above equation means that Δ_i corresponding to a_{coll} has to be determined for a given z_i from equation (17). In the case of $w = -1$ the problem can be reduced to solving equation (34) with s_{ta} given by equation (22). For other values of w we solve equation (17) iteratively finding Δ_i from the condition $s(a_{\text{ta}}) = s_{\text{ta}}$ where s_{ta} is given by equation (22) or (23). The procedure is simpler to perform if we combine equations (17) and (2) to obtain

$$\frac{ds}{da} = \frac{H_i}{H_0} \frac{f(a)}{g(a, s)} \quad (48)$$

and solve for $s(a)$ instead of $s(t)$. Equation (48) can be rewritten in the form of an integral equation

$$s(a) = 1 + \frac{H_i}{H_0} \int_{a_i}^a \frac{f(a')}{g[a', s(a')]} da' \quad (49)$$

where we used the boundary condition $s(a_i) = 1$. The first approximation of the solution, $s_1(a)$ is obtained by assuming $s(a') = 1$ in the integrand and calculating the integral numerically for a number of values of a in the range between a_i and the chosen a_{ta} and fitting $s_1(a)$ with a polynomial. The n -th approximation, $s_n(a)$, is obtained by introducing $s_{n-1}(a')$ in the integrand of (49).

It turns out that for flat cosmological models, on which we focus here, for large enough Ω_0 and independently of z_i the formula (22) for s_{ta} works for finding the solutions $s(a)$ for all considered cases of $w = -1, -2/3$ and $-1/3$. However, when going down with Ω_0 (and keeping $\Omega_0 + q_0 = 1$) the value of Δ_i obtained approaches $\Delta_{i,\text{cr}}$ and reaches it at $\Omega_0 \approx 0.05$ in the case of $w = -2/3$ and $\Omega_0 \approx 0.17$ in the case of $w = -1/3$. For lower values of Ω_0 the second solution for s_{ta} , equation (23), has to be used to find $s(a)$. Then the ratio $\Delta_i/\Delta_{i,\text{cr}}$ increases again.

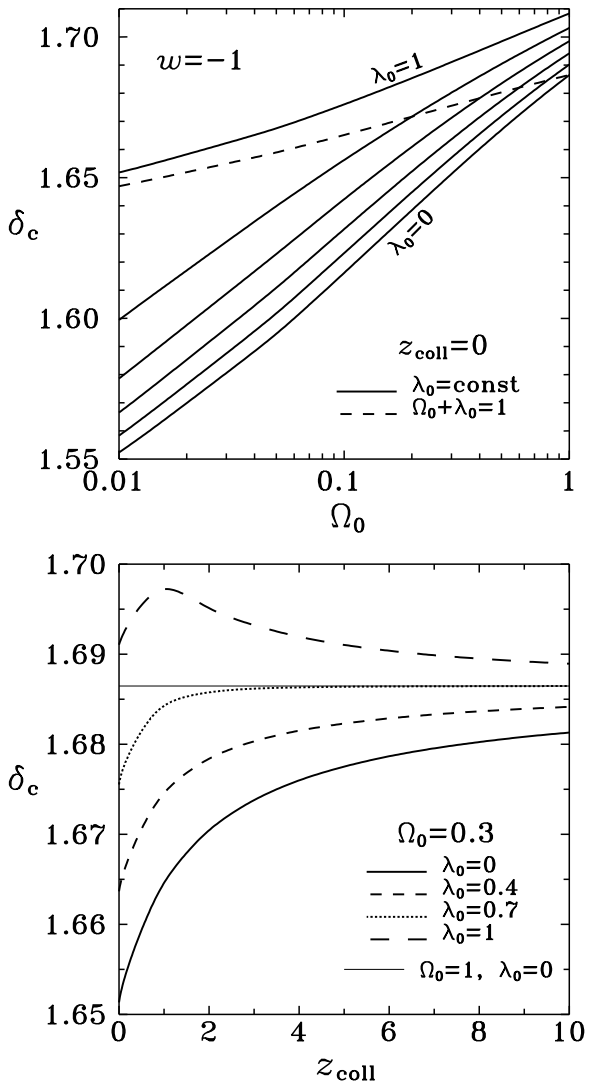


Figure 4. Parameter δ_c for $w = -1$. Upper panel: as a function of Ω_0 with solid lines corresponding from bottom to top to $\lambda_0 = 0, 0.2, 0.4, 0.6, 0.8, 1$ and the dashed line showing results for the flat case $\Omega_0 + \lambda_0 = 1$. Lower panel: as a function of z_{coll} for four models with $\Omega_0 = 0.3$ and $\lambda_0 = 0, 0.4, 0.7, 1$. The thin straight line marks the fiducial value $\delta_c = 1.68647$ for $\Omega_0 = 1, \lambda_0 = 0$.

Figure 4 shows δ_c calculated with $w = -1$. In the upper panel the assumption is that the collapse is taking place now, $z_{\text{coll}} = 0$. Solid lines display the dependence of δ_c on Ω_0 with $\lambda_0 = \text{const}$ while the dashed line has λ_0 chosen so that $\Omega_0 + \lambda_0 = 1$. In this last special case we reproduce the results of Eke, Cole & Frenk (1996), while for open models with no cosmological constant our results match those of Lacey & Cole (1993). Although it is not obvious from the Figure, for open models in the limit of $\Omega_0 \rightarrow 0$ we have $\delta_c \rightarrow 3/2$, independently of λ_0 .

The lower panel of Figure 4 shows how δ_c changes with the redshift of collapse, z_{coll} , for a few models with $\Omega_0 = 0.3$ and different values of λ_0 . We see that the dependence on z_{coll} is rather weak and at large z_{coll} the values converge to the well known fiducial value of $\delta_c = 3(12\pi)^{2/3}/20 \approx 1.68647$ valid in the Universe with $\Omega_0 = 1$ and $\lambda_0 = 0$. This value is

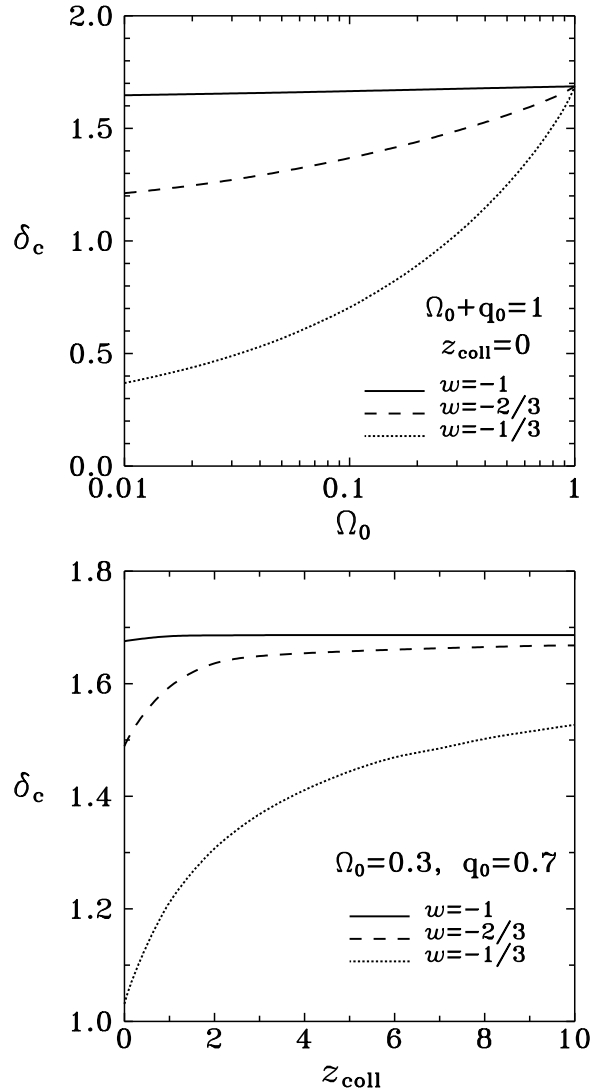


Figure 5. Parameter δ_c for three cases: $w = -1, -2/3$ and $-1/3$ as a function of Ω_0 for a flat Universe and $z_{\text{coll}} = 0$ (upper panel) and as a function of z_{coll} for $\Omega_0 = 0.3$ and $q_0 = 0.7$ (lower panel).

particularly quickly reached with increasing z_{coll} for the flat case, $\Omega_0 = 0.3, \lambda_0 = 0.7$.

Figure 5 compares results for δ_c with three different values of w for the flat model with $\Omega_0 + q_0 = 1$. As in Figure 4, the upper panel is for $z_{\text{coll}} = 0$, while the lower panel shows the dependence on z_{coll} for $\Omega_0 = 0.3$ and $q_0 = 0.7$. The dependence on w and Ω_0 turns out to be quite strong. We disagree on this point with the results of Wang & Steinhardt (1998) who claim to have found $1.6 < \delta_c < 1.686$ for all models.

4.2 The density of virialized halo

Another useful quantity is the ratio of the density in the object to the critical density at virialization

$$\Delta_c = \frac{\rho_{\text{vir}}}{\rho_{\text{crit}}}(a_{\text{coll}}) = \frac{\Omega(a_{\text{coll}})}{s_{\text{coll}}^3} \left(\frac{a_{\text{coll}}}{a_i} \right)^3 [1 + \Delta_i(a_{\text{coll}})] \quad (50)$$

where $s_{\text{coll}} = r_{\text{coll}}/r_i$ and r_{coll} is the effective final radius of the collapsed object. We assume that the object virializes at t_{coll} , the time corresponding to $s \rightarrow 0$. We first consider the case of $w = -1$. Application of the virial theorem in the presence of cosmological constant leads to the following equation for the ratio of the final radius of the object to its turn-around radius $F = r_{\text{coll}}/r_{\text{ta}}$ (Lahav et al. 1991)

$$2\eta F^3 - (2 + \eta)F + 1 = 0 \quad (51)$$

where

$$\eta = \frac{2\lambda_i s_{\text{ta}}^3}{\Omega_i(1 + \Delta_i)}. \quad (52)$$

In the calculations of Δ_c we use the exact solution to equation (51) which in the case of $\lambda > 0$ can be written down using expression (22) with F instead of s_{ta} and $b_1 = 2\eta$, $b_2 = -(2 + \eta)$ and $b_3 = 1$. However, a good approximation is provided by $F \approx (1 - \eta/2)/(2 - \eta/2)$ (Lahav et al. 1991).

Figure 6 shows Δ_c for $w = -1$. The upper panel gives its values as a function of Ω_0 for models with different values of λ_0 with the assumption that the collapse occurs at $z_{\text{coll}} = 0$. The solid lines correspond to constant values of λ_0 while the dashed line has λ_0 chosen so that $\Omega_0 + \lambda_0 = 1$. Again, we agree with the results for the special cases of $\Omega_0 < 1$, $\lambda_0 = 0$ and $\Omega_0 + \lambda_0 = 1$ derived previously by Lacey & Cole (1993) and Eke et al. (1996) respectively.

We see that for a given Ω_0 lower λ_0 makes virialized objects denser with respect to critical density. It is interesting to note, however, that this relation is inverted for higher z_{coll} as proved by the lower panel of Figure 6, where we display the dependence of Δ_c on the redshift of collapse for a few models. Again, as in the case of δ_c , we observe that at high z_{coll} values of Δ_c approach the well known fiducial value of $\Delta_c = 18\pi^2 \approx 177.653$ valid for $\Omega_0 = 1$, $\lambda_0 = 0$ and the convergence is fastest for the flat case.

For models with quintessence application of the virial theorem gives the following relation between the kinetic and potential energies at collapse

$$T_{\text{coll}} = -\frac{1}{2}W_{\text{G},\text{coll}} + W_{\text{Q},\text{coll}} \quad (53)$$

where W_{G} and W_{Q} are respectively the gravitational potential energy and the potential energy due to quintessence

$$W_{\text{G}} = -\frac{3}{5}\frac{GM^2}{r} \quad (54)$$

$$W_{\text{Q}} = -\frac{3}{10}H^2qMr^2. \quad (55)$$

Equating the total energies of the overdense region at turn-around and collapse

$$E_{\text{ta}} = W_{\text{G},\text{ta}} + W_{\text{Q},\text{ta}} \quad (56)$$

$$E_{\text{coll}} = T_{\text{coll}} + W_{\text{G},\text{coll}} + W_{\text{Q},\text{coll}} \quad (57)$$

$$= \frac{1}{2}W_{\text{G},\text{coll}} + 2W_{\text{Q},\text{coll}}$$

(where we used equation [53]) we obtain the equation for the collapse factor F

$$2\eta F^3 - \left[2 + \eta \left(\frac{a_{\text{coll}}}{a_{\text{ta}}} \right)^{3(1+w)} \right] F + 1 = 0 \quad (58)$$

with

$$\eta = \frac{2q_i s_{\text{ta}}^3}{\Omega_i(1 + \Delta_i)} \left(\frac{a_i}{a_{\text{coll}}} \right)^{3(1+w)}. \quad (59)$$

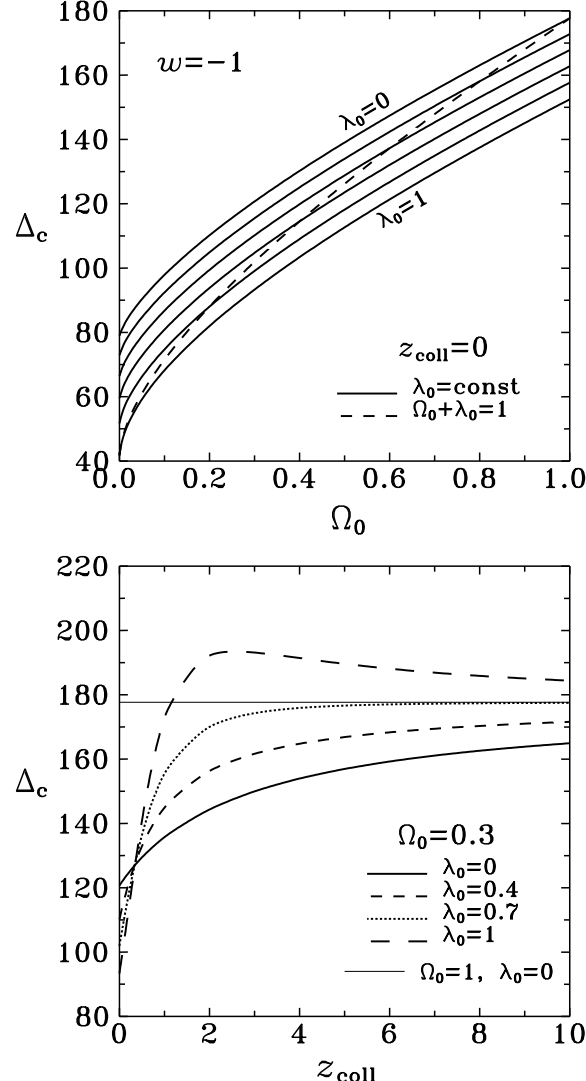


Figure 6. Parameter Δ_c for $w = -1$. Upper panel: as a function of Ω_0 with solid lines corresponding from top to bottom to $\lambda_0 = 0, 0.2, 0.4, 0.6, 0.8, 1$ and the dashed line showing results for the flat case $\Omega_0 + \lambda_0 = 1$. Lower panel: as a function of z_{coll} for four models with $\Omega_0 = 0.3$ and $\lambda_0 = 0, 0.4, 0.7, 1$. The thin straight line marks the fiducial value $\Delta_c = 177.653$ for $\Omega_0 = 1$, $\lambda_0 = 0$.

The exact solution to equation (58) is obtained in a similar way as in the case of cosmological constant.

Figure 7 compares results for Δ_c for three different values of w for the flat case of $\Omega_0 + q_0 = 1$. As in Figure 6, the upper panel is for $z_{\text{coll}} = 0$, while the lower panel shows the dependence on z_{coll} for $\Omega_0 = 0.3$ and $q_0 = 0.7$.

5 CHARACTERISTIC REDSHIFTS

It is sometimes useful to be able to estimate the redshift of a particular stage of evolution of the perturbation given its present overdensity as predicted by linear theory, $\delta_L(a = 1) = \delta_0$. For the redshift of collapse combining equations (46) and (47) we obtain

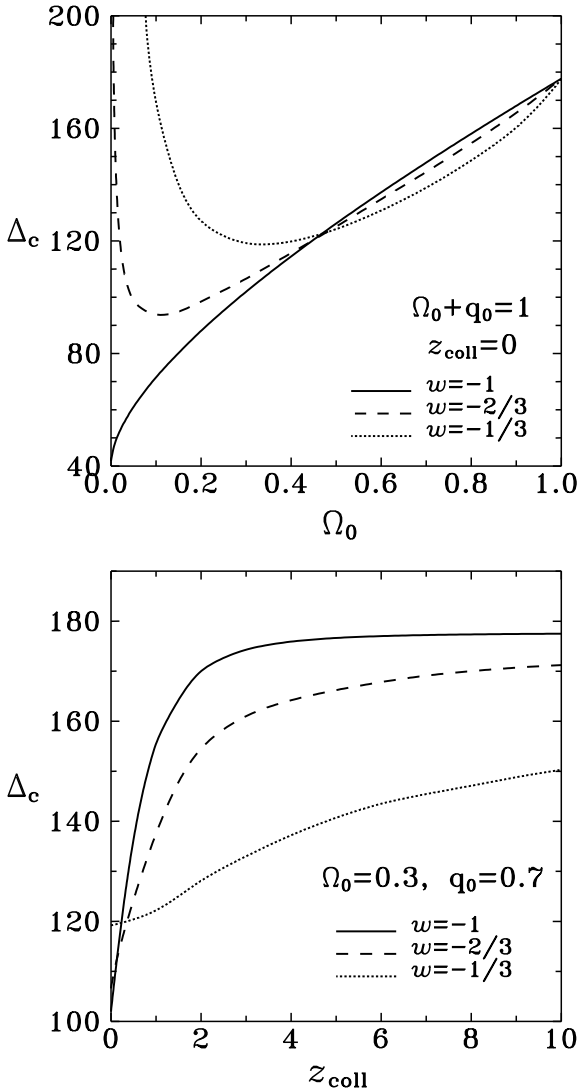


Figure 7. Parameter Δ_c for three cases: $w = -1, -2/3$ and $-1/3$ as a function of Ω_0 for a flat Universe and $z_{\text{coll}} = 0$ (upper panel) and as a function of z_{coll} for $\Omega_0 = 0.3$ and $q_0 = 0.7$ (lower panel).

$$\delta_0 = \delta_c(a_{\text{coll}}) \frac{D(a=1)}{D(a_{\text{coll}})}. \quad (60)$$

Using the previously obtained results for δ_c and appropriate formulae for the linear growth of fluctuations (12), (13) or (11), we can calculate the present linear density contrast of fluctuation that collapsed at z_{coll} . This relation can only be inverted analytically in the case of $\Omega_0 = 1, \lambda_0 = 0$ when we get $z_{\text{coll}} = \delta_0/\delta_c - 1$. For other cases the calculations have to be done numerically.

Using equation analogous to (60) we can also calculate the redshift of turn-around, z_{ta} . Parameter $\delta_c(a_{\text{coll}})$ has then to be replaced by the corresponding turn-around value $\delta_{\text{ta}}(a_{\text{ta}})$ which we do not give here, but which is calculated numerically from equation (33) or (49). δ_{ta} is close to unity for all models except for $w = -1/3$, where it is slightly lower at low redshifts.

Another interesting epoch in the evolution of an over-dense region is the onset of nonlinearity, which we character-

Table 1. Values of the best-fitting parameters α and β of equation (61) for $\Omega_0 = 0.3, q_0 = 0.7$.

w	z	α	β	accuracy
-1	z_{coll}	0.774	1.15	3 %
	z_{ta}	1.25	1.30	5 %
	z_{nl}	2.32	1.15	3 %
-2/3	z_{coll}	0.895	1.24	2 %
	z_{ta}	1.43	1.31	3 %
	z_{nl}	2.66	1.28	2 %
-1/3	z_{coll}	1.32	1.37	1 %
	z_{ta}	2.12	1.45	1 %
	z_{nl}	3.85	1.53	0.5 %

ize here by redshift z_{nl} . This is the time when the nonlinear density contrast given by equation (36) reaches unity. Again for the cosmological constant case equation equivalent to (60) can be used with δ_c replaced by $\delta_{\text{nl}}(a_{\text{nl}})$, which turns out to be of the order of 0.5. We obtain δ_{nl} from equation (33) replacing a_{ta} and s_{ta} by a_{nl} and s_{nl} where a_{nl} and s_{nl} obey equation (36) with $\delta = 1$. For quintessence models the calculations are made by constraining equation (49) in a similar way.

The resulting relations between the characteristic redshifts and δ_0 are shown in Figures 8 and 9. Figure 8 presents z_{coll} , z_{ta} and z_{nl} as functions of δ_0 for different models with $\Omega_0 = 0.3$ and cosmological constant $\lambda_0 = 0, 0.4, 0.7$ and 1. Figure 9 shows similar results for flat quintessence models with $\Omega_0 = 0.3, q_0 = 0.7$ and different w . The thin solid line in each panel of the two Figures gives for reference the exactly linear relation in the fiducial case of $\Omega_0 = 1, q_0 = 0$.

Figures 8 and 9 suggest that the dependence of characteristic redshifts on δ_0 can be well fitted with simple linear formulae

$$z = \alpha \delta_0 - \beta \quad (61)$$

where different constants α and β correspond to each of the three characteristic redshifts. In the $\Omega_0 = 1, \lambda_0 = 0$ model this relation is exact, we have $\beta = 1$ and $\alpha_{\text{coll}} = 1/\delta_c$, $\alpha_{\text{ta}} = 1/\delta_{\text{ta}}$, $\alpha_{\text{nl}} = 1/\delta_{\text{nl}}$. For the most popular flat Universe with $\Omega_0 = 0.3$ and $q_0 = 0.7$ we find the best fitting parameters α and β shown in Table 1. The fits are intended to be useful at high redshifts where the relation between z and δ_0 is almost exactly linear. The accuracy of the fits in terms of z obtained for a given δ_0 for $z > 1$ is shown in the last column of the Table. It should be emphasized that for high redshifts the fitted values of α and β work much better than δ_c , δ_{ta} , δ_{nl} and $\beta = 1$.

6 APPLICATION TO MASS FUNCTIONS

One of the most frequent applications of the spherical collapse model is to predict the mass function of bound objects using the PS formalism. According to their prescription the cumulative mass function (the comoving number density of objects of mass greater than M) is $N(> M) = \int_M^\infty n(M) dM$ where $n(M)$ is the number density of objects with mass between M and $M + dM$

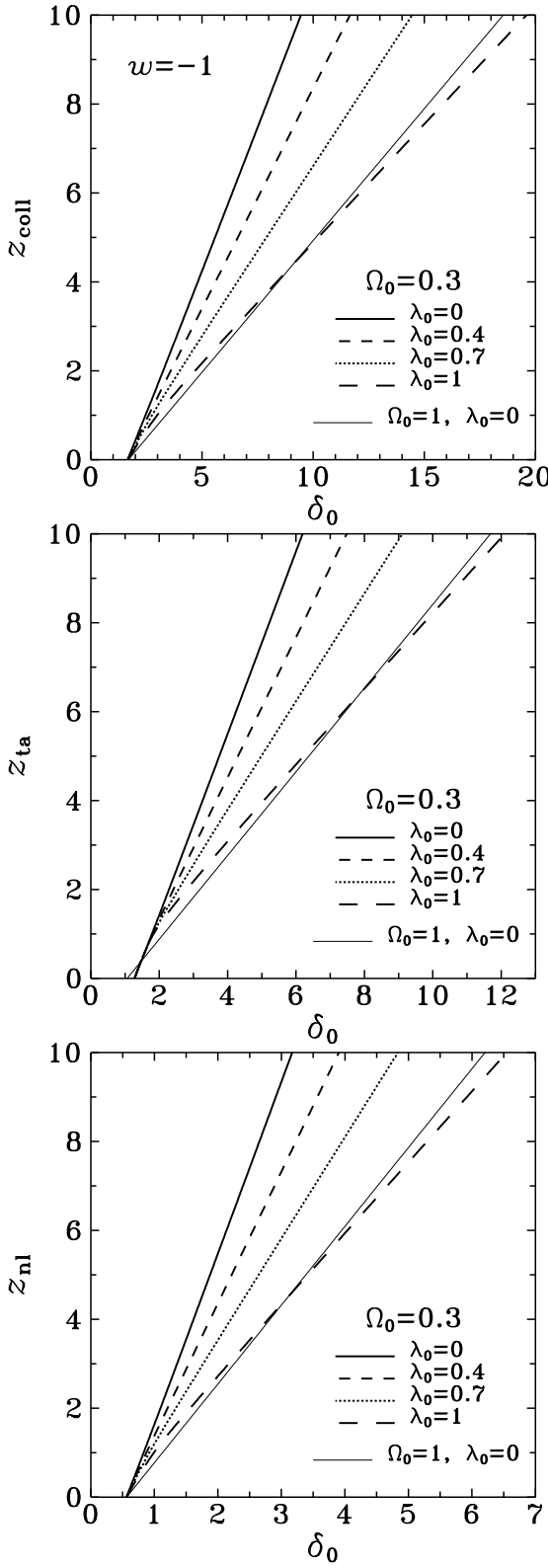


Figure 8. Redshift of collapse (upper panel), turn-around (middle panel) and transition to nonlinearity (lower panel) of density fluctuation with present linear density contrast δ_0 for four models with $\Omega_0 = 0.3$ and $\lambda_0 = 0, 0.4, 0.7$ and 1. The thin straight line in each panel marks the fiducial case of $\Omega_0 = 1, \lambda_0 = 0$.

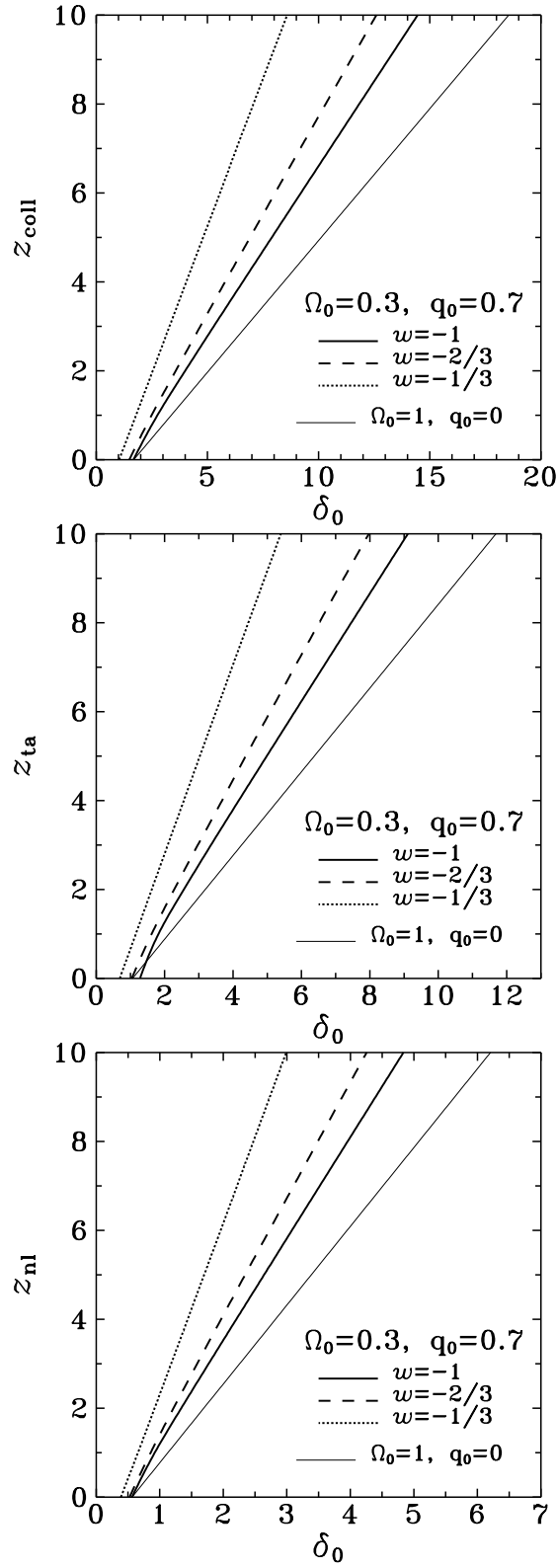


Figure 9. Redshift of collapse (upper panel), turn-around (middle panel) and transition to nonlinearity (lower panel) of density fluctuation with present linear density contrast δ_0 for three models $w = -1, -2/3$ and $-1/3$ with $\Omega_0 = 0.3$ and $q_0 = 0.7$. The thin straight line in each panel marks the fiducial case of $\Omega_0 = 1, q_0 = 0$.

$$n(M) = -\left(\frac{2}{\pi}\right)^{1/2} \frac{\varrho_b}{M} \frac{\delta_c}{\sigma^2} \frac{d\sigma}{dM} \exp\left(-\frac{\delta_c^2}{2\sigma^2}\right). \quad (62)$$

In the expression above, ϱ_b is the background density, δ_c is the characteristic density discussed in Subsection 4.1 and given by equation (47), σ is the rms density fluctuation at comoving smoothing scale R

$$\sigma^2 = \frac{1}{(2\pi)^3} \int d^3k P(k, a) W_{TH}^2(kR) \quad (63)$$

where the smoothing is performed with the top hat filter

$$W_{TH}^2(kR) = \frac{3}{(kR)^2} \left(\frac{\sin kR}{kR} - \cos kR \right). \quad (64)$$

The mass is then related to the smoothing scale by $M = 4\pi\varrho_b R^3/3$.

$P(k, a)$ in equation (63) is the power spectrum of density fluctuations which we assume here to be given in the form proposed by Ma et al. (1999) for flat models. For the present time ($a = 1$) the power spectrum is given by

$$P(k) = Ak^n T^2(k) \quad (65)$$

where n measures the slope of the primordial power spectrum (we will assume $n = 1$) and T is the transfer function. For the case of pure cosmological constant (Λ CDM) we take the transfer function T_Λ from Efstathiou, Bond and White (1992) with $\Gamma = \Omega_0 h$ and $h = 0.7$. For models with quintessence the transfer function in equation (65) is $T_Q = T_{Q\Lambda} T_\Lambda$, where $T_{Q\Lambda} = T_Q/T_\Lambda$ is approximated by fits given in Ma et al. (1999). We also adopt their COBE normalization of the spectra.

Figure 10 shows the cumulative mass functions calculated from equation (62) with $\Omega_0 = 0.3$ and $q_0 = 0.7$ for three models with $w = -1, -2/3$ and $-1/3$. The normalization constants for these three cases were respectively $A = 3.74 \times 10^6, 2.62 \times 10^6$ and $8.53 \times 10^5 (h^{-1}\text{Mpc})^4$, while the rms fluctuations at the scale of $8h^{-1}\text{Mpc}$ turn out to be $\sigma_8 = 1.12, 0.935$ and 0.534 . The parameters $\delta_c = 1.68, 1.49$ and 1.03 from Figure 5 were used. On top of the curves we plot the data points with $1-\sigma$ error bars obtained for clusters of richness class $R \geq -1$ by Girardi et al. (1998). Only the six data points for masses $M > 4 \times 10^{14} h^{-1} M_\odot$ are shown which are supposed to be free from the effect of incompleteness.

Comparison of the data points with the theoretical curves in Figure 10 clearly shows that for our choice of cosmological parameters the values of w close to $-2/3$ are preferred, in agreement with other tests (see e.g. Huterer & Turner 2000). However, the result should be treated with caution for at least three reasons. First, our choice of cosmological parameters, although well motivated by current data (see Harun-or-Rashid & Roos 2001 and references therein) is only one of many possible and it remains to be checked how the mass functions change when the parameters vary (for the discussion of a few models see Rahman & Shandarin 2001). Second, unfortunately, for larger masses where the three predictions start to differ significantly, the error bars of the data are much larger. Third, the region of larger masses (say, $M > 10^{15} h^{-1} M_\odot$) is also the region where the PS mass function is less reliable and when compared to the results of N-body simulations significantly underestimates the cumulative mass function (Jenkins et al. 2001).

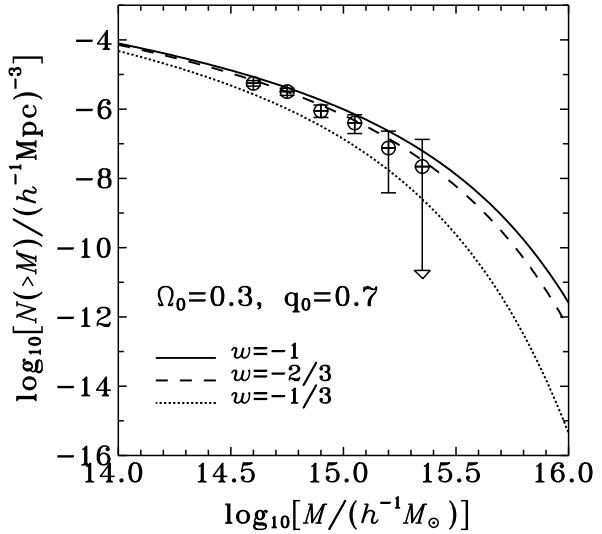


Figure 10. The PS cumulative mass functions for different w assuming $\Omega_0 = 0.3$ and $q_0 = 0.7$. The symbols mark the data for clusters from Girardi et al.

Rahman & Shandarin (2001) compared predictions of two alternatives to PS prescription, namely the analytic approximations given by Lee & Shandarin (1999) and Sheth & Tormen (1999). Of those three approximations, for all cosmological models considered the PS function gives always the lowest estimate of the mass function in the interesting mass range while the Lee-Shandarin formula gives the highest. Both those improved versions have their coefficients fixed by comparison with N-body simulations. Such simulations for models including quintessence have up till now been performed only for the $w = -2/3$ case (Bode et al. 2001) with the result similar as in other cosmological models: the PS function underestimates the mass function in the mass range considered. If the result holds for other values of w as well, the “true” predictions in Figure 10 would be shifted to higher number densities and still higher values of w would be preferred by the data.

7 DISCUSSION

The top hat model has been extended here to the case of the cosmological constant and quintessence models, including non-flat cosmologies. In particular, we have calculated the critical (over)density for collapse, the virial density and the characteristic redshifts of the collapse process. These include the redshifts of the transition to nonlinearity, turn-around and the collapse epoch. The characteristic redshifts cannot be represented by closed analytical expressions and therefore simple fitting formulae have been provided.

The top hat model constitutes the basic tool used in analytical and semi-analytical models of large scale structure and galaxy formation. The prime example here is the calculation of the mass function of collapsed objects by the PS formalism and its recent extensions (Lacey & Cole 1993; Somerville & Kolatt 1999). The PS mass function has a Gaussian term of the critical (over)density for collapse and

therefore an exact evaluation of this density should be used. Another important application of the top hat model is the semi-analytical modelling of galaxy formation (Kauffmann et al. 1999; Somerville and Primack 1999). The virial parameters of collapsed objects and the properties of baryons within such objects are often calculated in the framework of the top hat model, and this depends crucially on the background cosmologies.

We presented here an application of the top hat model calculations to the derivation of PS mass function of rich clusters of galaxies. Comparison of the results to the data of Girardi et al. (1998) indicates a preference of a flat $w = -2/3$ quintessence model over a flat cosmological constant dominated Universe.

ACKNOWLEDGEMENTS

We are grateful to M. Girardi for providing the data for the mass function of clusters in numerical form. This work was supported by the Polish KBN grant 2P03D02319 and by the Israel Science Foundation grant 103/98.

REFERENCES

Balbi A., Baccigalupi C., Matarrese S., Perrotta F., Vittorio N., 2001, *ApJ*, 547, L89

Barger V., Marfatia D., 2001, *Phys. Lett. B*, 498, 67

Bode P., Bahcall N. A., Ford E. B., Ostriker J. P., 2001, *ApJ*, 551, 15

Caldwell R. R., Dave R., Steinhardt P. J., 1998, *Phys. Rev. Lett.*, 80, 1582

Carroll S. M., Press W. H., Turner E. L., 1992, *ARAA*, 30, 499

Doran M., Lilley M. J., Schwindt J., & Wetterich, C., 2000, *ApJ*, in press, *astro-ph/0012139*

Efstathiou G., Bond J. R., White S. D. M., 1992, *MNRAS*, 258, 1P

Eke V. R., Cole S., Frenk C. S., 1996, *MNRAS*, 282, 263

Girardi M., Borgani S., Giuricin G., Mardirossian F., Mezzetti M., 1998, *ApJ*, 506, 45

Gunn J. E., 1977, *ApJ*, 218, 592

Gunn J. E., Gott J. R., 1972, *ApJ*, 176, 1

Hamilton A. J. S., 2001, *MNRAS*, 322, 419

Harun-or-Rashid S. M., Roos M., 2001, *A&A*, 373, 369

Heath D. J., 1977, *MNRAS*, 179, 351

Hoffman Y., Shaham J., 1985, *ApJ*, 297, 16

Huterer D., Turner M. S., 2000, *Phys. Rev. D*, submitted, *astro-ph/0012510*

Jenkins A., Frenk C. S., White S. D. M., Colberg J. M., Cole S., Evrard A. E., Couchman H. M. P., Yoshida N., 2001, *MNRAS*, 321, 372

Kauffmann G., Colberg J. M., Diaferio A., White S. D. M., 1999, *MNRAS*, 307, 529

Lacey C., Cole S., 1993, *MNRAS*, 262, 627

Lacey C., Cole S., 1994, *MNRAS*, 271, 676

Lahav O., Lilje P. B., Primack J. R., Rees M. J., 1991, *MNRAS*, 251, 128

Lee J., Shandarin S. F., 1999, *ApJ*, 500, 14

Lokas E. L., 2000, *MNRAS*, 311, 423

Lokas E. L., Hoffman Y., 2001, in Spooner N. J. C., Kudryavtsev V., eds, Proc. 3rd International Workshop, The Identification of Dark Matter. World Scientific, Singapore, p. 121, *astro-ph/0011295*

Ma C. P., Caldwell R. R., Bode P., Wang L., 1999, *ApJ*, 521, L1

Maor I., Brustein R., Steinhardt P. J., 2001, *Phys. Rev. Lett.*, 86, 6

Martel H., 1991, *ApJ*, 377, 7

Peebles P. J. E., 1980, The Large-Scale Structure of the Universe. Princeton Univ. Press, Princeton, NJ

Press W. H., Schechter P., 1974, *ApJ*, 187, 425 (PS)

Rahman N., Shandarin S. F., 2001, *ApJ*, 550, L121

Ratra B., Peebles P. J. E., 1988, *Phys. Rev. D*, 37, 3406

Sheth R., Tormen G., 1999, *MNRAS*, 308, 119

Somerville R. S., Kolatt T. S., 1999, *MNRAS*, 305, 1

Somerville R. S., Primack J. R., 1999, *MNRAS*, 310, 1087

Steinhardt P. J., Wang L., Zlatev I., 1999, *Phys. Rev. D*, 591, 270

Wang L., Steinhardt P. J., 1998, *ApJ*, 508, 483

Wang L., Caldwell R. R., Ostriker J. P., Steinhardt P. J., 2000, *ApJ*, 530, 17

Weinberg S., 1987, *Phys., Rev. Lett.*, 59, 2607

Weller J., Albrecht A., 2001, *Phys., Rev. Lett.*, 86, 1939

Zlatev I., Wang L., Steinhardt P. J., 1999, *Phys. Rev. Lett.*, 82, 896